Molecular Therapy
Oncolytics
Original Article

A host non-coding RNA, nc886, plays a pro-viral role by promoting virus trafficking to the nucleus

Enkhjin Saruuldalai,[1] Jiyoung Park,[2] Dongmin Kang,[2] Seung-Phil Shin,[3] Wonkyun Ronny Im,[1] Hwi-Ho Lee,[1] Jiyoung Joan Jang,[1] Jong-Lyul Park,[4,5] Seon-Young Kim,[4,5] Jung-Ah Hwang,[6] Young-Dong Kim,[7,8] Jung-Hoon Lee,[8] Eun Jung Park,[1] Yeon-Su Lee,[9] In-Hoo Kim,[1] Sang-Jin Lee,[3] and Yong Sun Lee[1]

[1]Department of Cancer Biomedical Science, Graduate School of Cancer Science and Policy, National Cancer Center, Goyang 10408, Korea; [2]Fluorescence Core Imaging Center, Department of Life Science, Ewha Womans University, Seoul 03760, Korea; [3]Division of Cancer Immunology, Research Institute, National Cancer Center, Goyang 10408, Korea; [4]Personalized Genomic Medicine Research Center, KRIBB, Daejeon 34141, Korea; [5]Department of Functional Genomics, University of Science and Technology, Daejeon 34113, Korea; [6]Genomics Core Facility, Research Core Center, Research Institute, National Cancer Center, Goyang 10408, Korea; [7]Department of Life Science, Hallym University, Chuncheon 24252, Korea; [8]Multidisciplinary Genome Institute, Hallym University, Chuncheon 24252, Korea; [9]Division of Clinical Cancer Research, Research Institute, National Cancer Center, Goyang 10408, Korea

Elucidation of the interplay between viruses and host cells is crucial for taming viruses to benefit human health. Cancer therapy using adenovirus, called oncolytic virotherapy, is a promising treatment option but is not robust in all patients. In addition, inefficient replication of human adenovirus in mouse hampered the development of an *in vivo* model for preclinical evaluation of therapeutically engineered adenovirus. nc886 is a human non-coding RNA that suppresses Protein Kinase R (PKR), an antiviral protein. In this study, we have found that nc886 greatly promotes adenoviral gene expression and replication. Remarkably, the stimulatory effect of nc886 is not dependent on its function to inhibit PKR. Rather, nc886 facilitates the nuclear entry of adenovirus via modulating the kinesin pathway. nc886 is not conserved in mouse and, when xenogeneically expressed in mouse cells, promotes adenovirus replication. Our investigation has discovered a novel mechanism of how a host ncRNA plays a pro-adenoviral role. Given that nc886 expression is silenced in a subset of cancer cells, our study highlights that oncolytic virotherapy might be inefficient in those cells. Furthermore, our findings open future possibilities of harnessing nc886 to improve the efficacy of oncolytic adenovirus and to construct nc886-expressing transgenic mice as an animal model.

INTRODUCTION

When viruses infect host cells, the fate of a virus as well as the clinical outcome of hosts is mainly determined by genetic and epigenetic factors of infected cells. Recently, a growing number of studies have reported evidence for the role of non-coding RNAs (ncRNAs) therein. Most of them are about microRNAs and long ncRNAs. Unraveling the interplay between viruses and host cells is crucial in preventing or treating virus infection itself and related diseases. Furthermore, we could reprogram a virus for our benefit in clinics. A prominent example is adenovirus (AdV), which has been widely used in oncolytic virotherapy (reviewed in Jounaidi et al[1]) and gene therapy (reviewed in Lee et al[2]).

Human AdV is a non-enveloped virus with a double-stranded linear DNA genome (reviewed in Jounaidi et al[1] and Mennechet et al[3]). Upon entry into cells via interaction with cell surface receptors and attachment factors, AdV particles traverse through the cytoplasm along microtubules, to inject AdV DNA into the nucleus (reviewed in Wolfrum and Greber[4] and Pied and Wodrich[5]). Therein, the transcription of AdV occurs temporally to express early and late genes by host RNA polymerases. Among a total of 30 to 40 AdV genes, most of them are protein-coding genes and are transcribed by RNA polymerase II (Pol II), while two ncRNAs are transcribed by RNA polymerase III (Pol III). These are called virus-associated (VA) RNAs, which are expressed in all human AdV serotypes[6] and essential for efficient AdV replication (reviewed in Vachon and Conn[7]). The viral gene expression is followed by assembly of progeny virions and release of them accompanying cell lysis.

A clinical utility of AdV is based on cell lysis at the final stage of its life cycle. AdV prefers proliferating cells for its propagation.[8] In addition, the interferon signaling is usually compromised in cancer cells.[9,10] These facts provided a rationale for AdV to kill cancer cells preferentially (called "oncolytic virotherapy"; reviewed in Baker et al[11]). Owing to extensive knowledge on AdV biology, AdV has been subjected to genetic modification for development of more selective oncolytic agents to tumor cells. Nonetheless, a basic setback is that the AdV-mediated oncolytic virotherapy is not effective in all cancer cells. It has been noted that approximately one-third of patients treated with AdV exhibited no response.[1,12] In addition, human AdVs replicate inefficiently in mice,[13–16] which makes it challenging to construct an appropriate *in vivo* model to assess effectiveness of oncolytic AdV for therapeutic purpose.

Received 3 September 2021; accepted 15 February 2022;
https://doi.org/10.1016/j.omto.2022.02.018.

Correspondence: Yong Sun Lee, Department of Cancer Biomedical Science, Graduate School of Cancer Science and Policy, National Cancer Center, Goyang 10408, Korea.
E-mail: yslee@ncc.re.kr

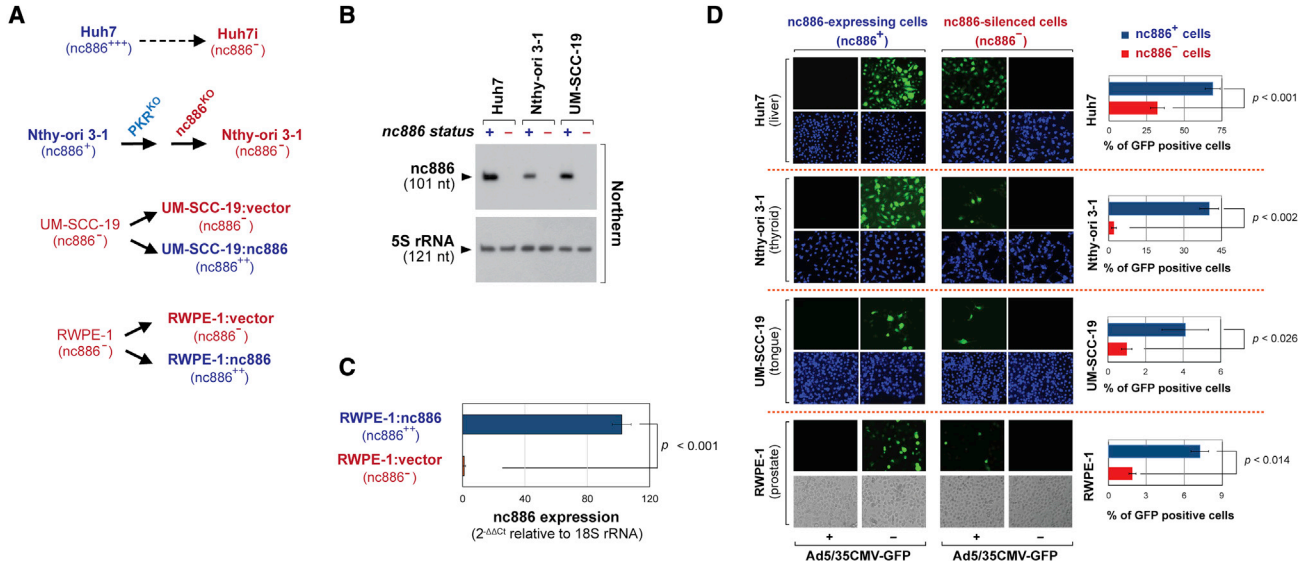

Figure 1. nc886 promotes gene expression from infected AdV

(A) A diagram depicting cell lines used in (B–D). Dotted and solid arrows indicate fortuitous derivation and experimental production, respectively. Relative nc886 expression levels are designated by a superscripted hyphen (silenced expression) and number of + (with +++ being the highest). nc886^{+} (red letters) and nc886^{-} (blue letters) pairs that were actually used in (B–D) are bold-highlighted. (B) Northern hybridization of nc886 and 5S rRNA to ensure equal loading. (C) RT-qPCR of nc886. The normalized value (to 18S rRNA) of RWPE-1:vector was set as 1. (D) GFP signal upon Ad5/35CMV-GFP infection, with DAPI staining (for Huh7, Nthy-ori 3-1, and UM-SCC-19) or cell photo (for RWPE-1). GFP positive cells were counted and their percentage out of total cells (from DAPI or cell images) are plotted on the right. Infection dose and detection time are 10 MOI at 24 h post-infection (Huh7), 20 MOI at 24 h (Nthy-ori 3-1), and 20 MOI at 48 h (UM-SCC-19 and RWPE-1).

nc886 is a human ncRNA that is transcribed by Pol III and modulates the activity of target proteins.[17–19] The established function of nc886 is to repress the activity of an antiviral protein called Protein Kinase R (PKR).[17,20–22] VA RNAs, Pol III transcripts of AdV, also suppress PKR.[7] It is intriguing that nc886, a host-encoded ncRNA, shares similar properties with AdV ncRNAs. In addition, the interplay between nc886 and virus has been reported in a few studies. nc886 expression is increased upon infection of Epstein-Barr virus and influenza A virus.[23–25] nc886 plays a stimulating role in propagation of influenza A virus.[25] All these facts prompted our curiosity as to whether nc886 plays a role during AdV infection. Here our study has uncovered the pro-AdV role of nc886 and its action mechanism.

RESULTS

nc886 promotes AdV gene expression

Since nc886 suppresses antiviral responses,[17,26] we hypothesized that nc886 would act in favor of AdV. To assess the role of nc886, we needed a pair of nc886-expressing and -deficient cells (designated nc886^{+} or nc886^{-} cells, respectively). Since nc886 plays roles in cell proliferation and apoptosis,[27,28] construction of nc886-expressing or knockout (KO) cells was not successful in all cell lines. Nonetheless, we collected a pair of nc886^{+} and nc886^{-} cells from four cell lines: Huh7, Nthy-ori 3-1, UM-SCC-19, and RWPE-1 (Figure 1A). A hepatoma cell line Huh7 expressed nc886 abundantly. While culturing Huh7 cells, we fortuitously obtained nc886^{-} cells and named them Huh7i. When gene expression profiles were analyzed, correlation between Huh7 and Huh7i was higher than that between any pair of unrelated cell lines (Figure S1). This ensured that Huh7i was a genuine derivative from Huh7 but a contaminant. Nthy-ori 3-1 is an immortalized thyroid cell line that expresses nc886. We had constructed an nc886^{-} cell line by sequential KO of PKR and nc886 in our previous study[29] (to be used in Figure 2 and later). UM-SCC-19 and RWPE-1 are cancer cell lines derived from tongue and prostate, respectively. Both of them were nc886-silenced. We constructed nc886-expressing derivative cell lines by transfecting a lentiviral plasmid harboring the nc886 gene. Corresponding control cell lines were also constructed via a parallel procedure with an empty vector. The scheme for cell line establishment is depicted in Figure 1A. The nc886 status was validated by Northern or RT-qPCR measurement (Figures 1B and 1C).

"Ad5/35CMV-GFP" is a modified AdV that is devoid of its early gene E1 but expresses GFP under the cytomegalovirus (CMV) promoter.[30] For GFP to be expressed, Ad5/35CMV-GFP should enter into cells upon attachment to the cell surface receptor CD46, the AdV genome should translocate to the nucleus, and AdV genes should be transcribed. So, GFP signal is indicative of how efficiently the AdV propagation cycle operates. The higher GFP signal in nc886^{+} cell lines than in nc886^{-} counterparts (Figure 1D) indicated that nc886 stimulates a step(s) of the AdV propagation cycle.

nc886 promotes AdV replication in a PKR-independent manner

As stated earlier, an established role of nc886 is to inhibit the activity of PKR, an antiviral protein.[31] So, it is plausible that the inhibition of PKR accounts for the stimulatory effect of nc886 on AdV. To test this

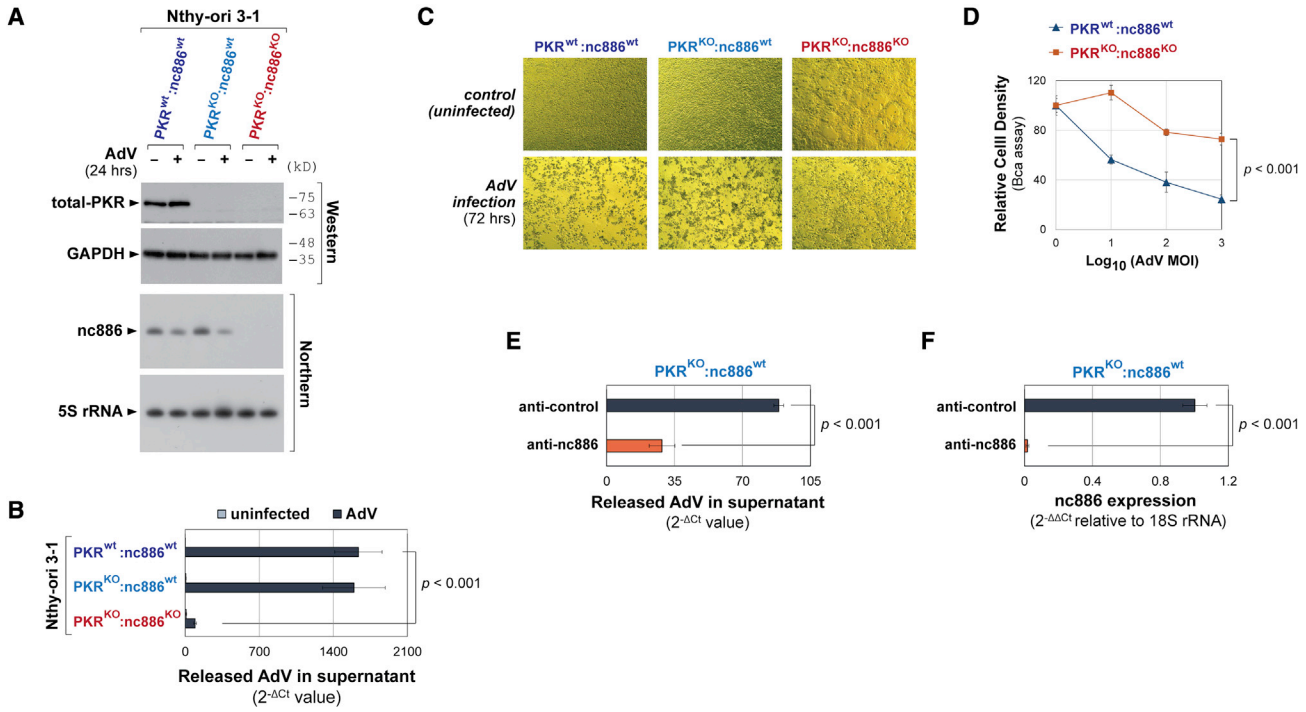

Figure 2. The impact of nc886 on AdV is independent of PKR

(A) AdV infected and uninfected control (designated as + and –, respectively) to Nthy-ori 3-1 and derivatives that were constructed sequentially as shown in Figure 1A. Infection was at 10 MOI in (B–F). Western blot of indicated proteins, with molecular size markers indicated on the right (top panels). Northern blot of nc886 and 5S rRNA (bottom panels). (B) qPCR of released progeny AdV DNA amounts at 24 h post-infection. An average and the standard deviation from triplicate samples are shown with a p value. (C) Cell photos at 72 h post-infection. (D) Measurement of cell numbers by BCA assay at 72 h post-infection. An absorbance value at 570 nm was converted to a cell density as described in materials and methods. The value of uninfected control was set 100 and relative values were plotted. Each value is an average of triplicates. Standard deviations and a p value are indicated. (E and F) qPCR of AdV from culture supernatant (E) upon infection of AdV (for 24 h) and transfection of indicated anti-oligonucleotides (for 22 h), as described in (B). Cells were harvested and RNA was isolated for RT-qPCR of nc886 (F).

possibility, we employed a set of cell lines that we constructed in our previous study.[29] Nthy-ori 3-1, an immortalized thyroid cell line, expresses PKR and nc886 (PKR^{wt}:$nc886^{wt}$ in Figure 2A). Since nc886 KO in the PKR wild-type (WT) background was deleterious due to PKR activation and the resultant apoptosis, we had sequentially made PKR and nc886 KO cell lines (PKR^{KO}:$nc886^{WT}$ and PKR^{KO}:$nc886^{KO}$) (Figure 2A). While validating the PKR and nc886 status, we found that nc886 expression declined at 24 h post-infection of AdV. Since AdV DNA was replicated and a huge quantity of VAI RNA was expressed at this time point (shown in Figures 3A–3C), the decrease of nc886 was most likely due to an ample copy number of VA promoters that titrated available Pol III enzymes away from the nc886 promoter.

We measured AdV DNA that was released into culture supernatant after completing AdV DNA replication and virion assembly. Importantly, AdV propagation was barely affected by PKR KO but was remarkably diminished upon nc886 KO (Figure 2B). Accordingly, the AdV-mediated cytotoxicity was much higher in nc886-expressing cells than in nc886 KO cells (Figures 2C and 2D).

Since nc886 KO cells were a selected clone, we had a concern about whether the dramatic decrease of AdV release and cytotoxicity might be attributed to a genetic or epigenetic alteration(s) other than nc886. To ensure that it is genuinely the effect pf nc886, we performed a short-term knockdown (KD) experiment by transfecting an anti-oligonucleotides targeting nc886 ("anti-nc886"). The released AdV was significantly diminished by "anti-nc886" as compared with "anti-control," a non-targeting anti-oligonucleotides (Figure 2E). Efficient KD was verified by RT-qPCR of nc886 (Figure 2F).

There were two points that should be underlined. First, PKR WT and KO cells yielded almost the same results. Second, more importantly, nc886 KO and KD experiments were done in the PKR KO cells. If PKR inhibition were critical for the effect of nc886 on AdV, there must have been no difference regardless of nc886 in the PKR-null situation because there was no PKR to inhibit. These data led to a conclusion that PKR itself did not obstruct AdV life cycle nor could account for the stimulatory effect of nc886 on AdV propagation.

The pro-AdV effect of nc886 operates at or prior to AdV early gene expression

As the first step toward elucidating a mechanism, we attempted to determine a stage(s) at which nc886 exerted its pro-AdV role. Briefly, sequential events in the AdV life cycle are (depicted in Figure 3A) as

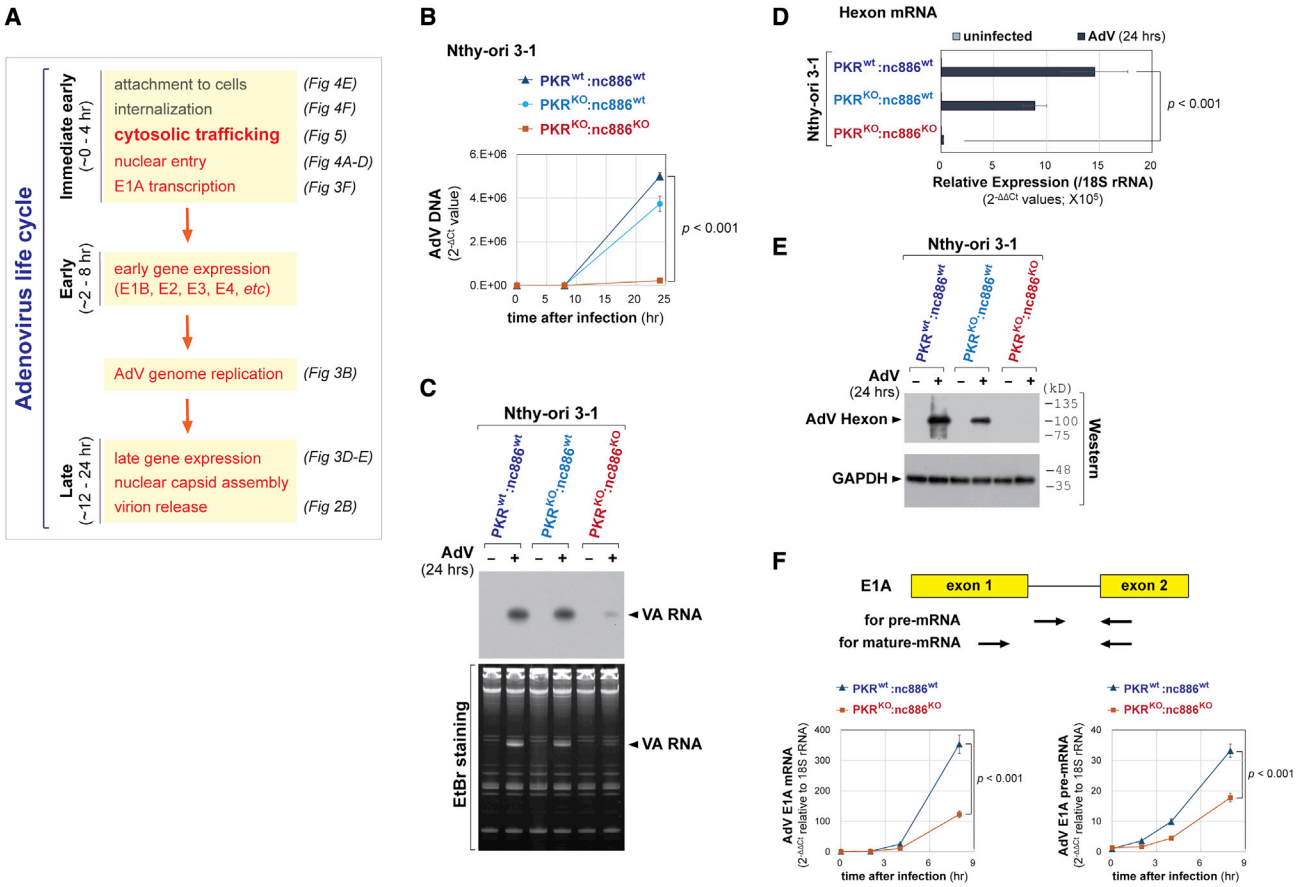

Figure 3. Effect of nc88 on AdV DNA replication and gene expression

(A) AdV infection timeline. To identify which step nc886 stimulates, we infected AdV (at 10 MOI unless specified otherwise) and conducted various assays at time points that are indicated in each figure. (B) qPCR of intracellular AdV DNA. qPCR Ct values were normalized to qPCR Ct values of 18S rDNA. (C) Northern hybridization of AdV VAI RNA. EtBr staining is shown for equal loading and also for highlighting the abundance of VAI RNA. (D and E) RT-qPCR and Western blot of hexon mRNA and protein. The GAPDH image is the same as Figure 2A, since this and Figure 2A experiments were done in a batch of infection and measurement. (F) RT-qPCR, using primers (indicated in upper panel), of AdV E1A mature mRNA (bottom left) and pre-mRNA (bottom right).

follows: attachment onto a cell surface receptor, entry into cells, traverse across the cytosol, release of AdV DNA into the nucleus, expression of the immediate-early gene E1A and early genes, AdV DNA replication, expression of late genes, and viral assembly and release (reviewed in Sohn and Hearing[32]).

First, we assessed the effect of nc886 on AdV DNA replication by measuring the intracellular copy number of AdV DNA. AdV DNA was barely detectable at 8 h but clearly seen at 24 h (Figure 3B). At 24 h in the absence of nc886, we observed severely impaired AdV DNA replication (Figure 3B) and accordingly very low expression of VAI RNA (Figure 3C). Although VAI is regarded to be an early gene, it is known to be transcribed also from ample copies of replicated AdV DNA. Actually, we observed its expression at 24 h, as huge as could be detectable even by ethidium bromide staining (Figure 3C, bottom panel). Second, we examined the expression of a late gene, hexon. The expression levels of hexon mRNA and protein were markedly decreased in nc886 KO cells as compared with nc886-expressing cells (Figures 3D and 3E). All these results indicated that nc886 acted at or prior to AdV replication.

We measured expression of the AdV immediate-early gene, E1A, at 8 h and earlier. The mature, spliced mRNA was substantially decreased upon nc886 KO (Figure 3F). mRNA maturation involves several post-transcriptional events, which might have been altered by nc886. To exclude these events, we conducted RT-qPCR with a primer pair that measured the precursor mRNA (pre-mRNA) (Figure 3F). The E1A pre-mRNA level was significantly lower in nc886 KO cells than in WT cells (Figure 3F). This lower expression was evidently seen as early as 2 h post-infection. Collectively from our data in Figures 2 and 3, we determined that nc886 promoted AdV at or prior to transcription of the immediate-early gene.

nc886 promotes nuclear entry of AdV DNA

There were two possibilities for the lower E1A pre-mRNA level in nc886 KO cells: a slower transcription rate or fewer AdV DNA

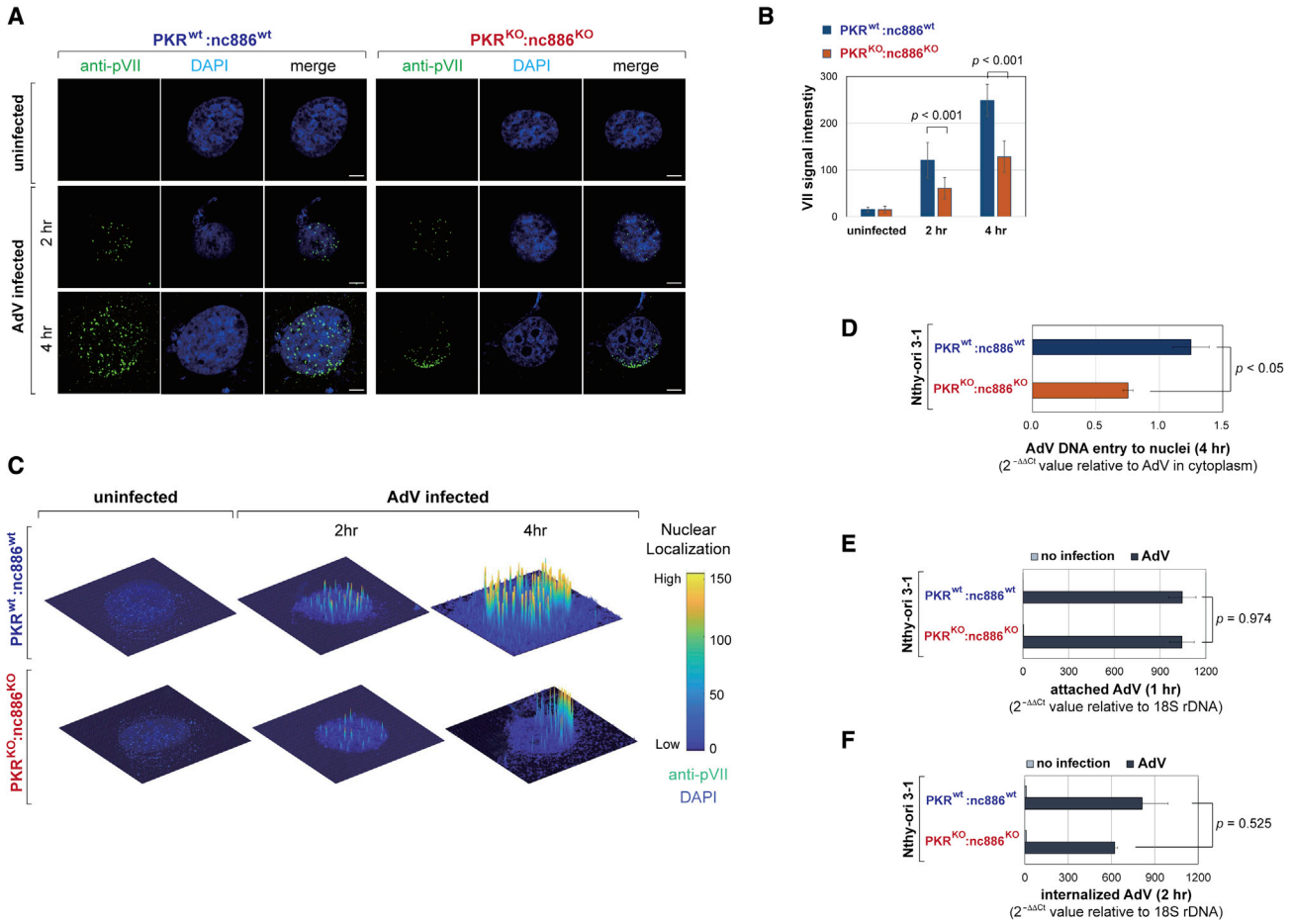

Figure 4. nc886 promotes nuclear entry of AdV DNA but not cellular entry

(A and B) IF of AdV protein VII (green), together with nuclei staining with DAPI (blue) at indicated times after infection of AdV at 50 MOI. Representative images are in (A) and quantitation is in (B). Signals were counted by using the Zen program (Carl Zeiss; Oberkochen, Germany). Each value is an average of three independent experiments (n = 15–18 cells examined for each experiment). Standard deviations and p values are indicated. (C) IF images of (A) were processed through the MATrix LABoratory (MATLAB) software for three-dimensional visualization. (D) qPCR of AdV DNA in isolated nuclei, at 4 h after AdV infection at 50 MOI. qPCR Ct values of nuclear AdV were normalized to those of corresponding cytoplasmic AdV. (E and F) qPCR of DNA isolated from attached and internalized AdV. qPCR Ct values were normalized to RT-qPCR Ct values of 18S rDNA.

molecules that are transcription templates in the nucleus. In the former possibility, we would search for a candidate transcription factor. In the latter possibility, we would further track back earlier steps in the AdV life cycle (see Figure 3A). To determine which was the case, we measured the nuclear amount of AdV DNA by immunofluorescence (IF) of AdV protein VII, a protein associated with the AdV genome. When AdV particles traverse the cytosol and reach the perinuclear region, the AdV capsid disintegrates and only the genomic DNA and associated proteins are released into the nucleus. During this course of events, the protein VII epitope is obscured by the capsid in the cytosol but is exposed only after release into the nucleus. Thus, the intensity of protein VII provides an alternative but apt indicator for the AdV DNA quantity in the nucleus.[5] Also in our IF experiment, protein VII signal was seen within DAPI staining (Figure 4A). Importantly, protein VII signal intensity was significantly weaker in nc886 KO cells than in WT cells (Figures 4A and 4B). The 2-fold difference in IF signal, a proxy of AdV DNA quantity, was concordant with our measurement of E1A pre-mRNA (Figure 3F). Figure 4A images left a slim possibility that the signal might have come from protein VII attached outside of the nuclear surface. To exclude this possibility, we processed the IF images for three-dimensional visualization to confirm intranuclear localization of protein VII signal (Figure 4C). Furthermore, we conducted biochemical fractionation to isolate nuclei and measured AdV DNA therein. This assay also showed an approximately 2-fold decrease of nuclear AdV DNA amount upon nc886 KO (Figure 4D). All these data suggested that nuclear import of the AdV genome was attenuated without nc886, which resulted in fewer DNA templates for E1A transcription.

nc886 does not affect AdV entry into cells

nc886 most likely took effect at a step before AdV nuclear import. Until AdV particles reach the nucleus, they undergo multiple

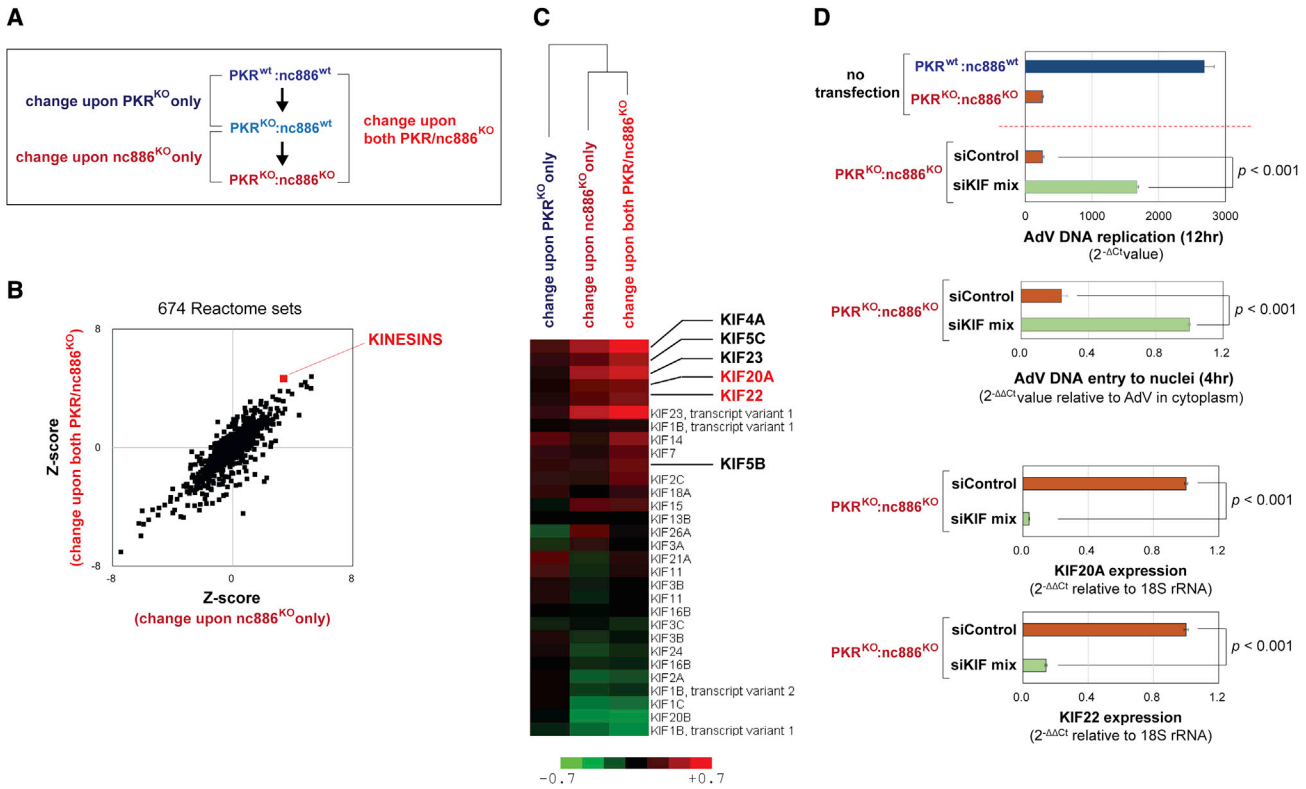

Figure 5. The elevated expression of kinesins is the reason for inefficient AdV replication in nc886 KO cells

(A) Nomenclature of comparison pairs for analysis of the Reactome pathway (B) and gene expression (C). (B) A scatterplot of *Z*-scores for 674 Reactome gene sets (see also Table S1) showing the correlation between two pairs. The pathway "KINESINS" is marked by a larger red square. (C) A heatmap depicting relative expression of 30 kinesin family genes selected from a total of 61 kinesin family members (see Table S2 and legend for the selection criterion). (D) KD of kinesin proteins. A mixture of siRNAs against KIF20A and KIF22 (40 nM each) was transfected into nc886 KO cells for 12 h, and then followed by AdV infection for 12 h for replicated AdV DNA measurement and 4 h for AdV DNA that entered to nuclei. Graphs are as follows: qPCR to measure replicated AdV DNA (top panel, the same experiment as Figure 3B), qPCR to measure AdV DNA that entered nuclei (middle panel, the same experiment as Figure 4D), and RT-qPCR for KIF20A and KIF22 expression to assess KD efficiency (bottom two panels).

interactions with host factors. The AdV journey to the nucleus can be briefly described as follows. The initial attachment to cell surface receptors leads to clathrin-mediated endocytosis. After escape from endosome, AdV particles associate with dynein motor proteins to travel along microtubules to the nuclear pore complex (reviewed in Greger and Flatt[33]). Among host factors related to above processes, we interrogated whether any of them was differentially expressed between nc886-expressing and -deficient cells, by performing nCounter analysis, which provided expression data on a set of mRNAs and proteins from a nanoString panel (Figure S2). In addition, we looked into our previous Illumina microarray data.[29] These analyses identified several candidate genes and pathways including epidermal growth factor receptor (EGFR), Rac Family Small GTPase 1 (RAC1), and the kinesin pathway (shown later in Figure 5). EGFR and RAC1 are implicated in uptake of several viruses[4,34]; kinesin proteins implicated in AdV cytoplasmic trafficking.[35]

We continued to trace stages of AdV infection retrospectively, by performing two experiments: attachment assay and internalization assay.[36] In the attachment assay, the mixture of AdV particles was kept for a short time at 4°C, in which condition AdV internalization was mostly blocked and thus we could measure the degree of AdV binding to the cell surface. The internalization assay measures only AdV particles inside cells, as there were multiple thorough washing steps to eliminate AdV on the cell surface. The amount of AdV particles on the cell surface was similar between nc886 WT and KO cells (Figure 4E). In line with this result, cell surface receptors were expressed both in nc886-expressing and KO cells to a comparable degree (Figure S3).

Since EGFR and RAC1 were one of the top suppressed genes upon nc886 KO (Figure S2), we expected that AdV entry to cells was defective in the absence of nc886. Against our expectation, our internalization assay showed no significant difference in the amount of internalized AdV particles (Figure 4F). This result was corroborated by IF of hexon, the major capsid protein, whose intracellular signal was comparable between nc886 WT and KO cells (Figure S4). Furthermore, inhibition of EGFR and RAC1 by small interfering RNA (siRNA) or chemical inhibitors did not decrease AdV replication in Nthy-ori 3-1 nc886 WT cells (E.S. and Y.S.L., unpublished data). Collectively, we concluded that nc886 did not affect AdV cellular entry.

The suppression of the kinesin pathway is the reason for the pro-AdV effect of nc886

We performed Reactome pathway analysis in the Molecular Signature Database (MSigDB; https://www.gsea-msigdb.org/gsea/msigdb/). Reactome is composed of 674 pathway sets and each set contains several tens to hundreds of genes whose overall change of their relative expression levels is expressed in Z-scores. Positive or negative *Z*-scores indicated whether a pathway is activated or suppressed, respectively. From pairwise comparisons of gene expression data, we obtained 674 *Z*-scores from "change upon nc886^{KO} only" and "change upon both PKR/nc886^{KO}" and plotted them (Figures 5A and 5B, Table S1). Most notably, the kinesin pathway ("KINESINS") was one of the most up-regulated ones in both the two pairwise comparisons (Figure 5B). It is also worth mentioning that Reactome *Z*-scores between "change upon nc886^{KO} only" and "change upon both PKR/nc886^{KO}" were positively correlated (Pearson's R value = +0.843, Figure 5B). Such a high correlation indicated that nc886 posed similar impact on gene expression regardless of whether the PKR status was WT or KO and that sole PKR KO had very modest impact on gene expression. Actually in our previous report, PKR KO *per se* did not result in any recognizable phenotypic change in an unstressed growing condition.[29]

Kinesins are a family of motor proteins moving along microtubules.[37] They move from the center of a cell to its periphery (called "plus end transport"), as opposed to dynein that is responsible for "minus end transport" of AdV. A recent work reported that KD of a handful of kinesin proteins leads to increase of AdV in the perinuclear region, implying antagonistic action of kinesins in AdV nuclear trafficking.[35] Thus, we hypothesized that the increase of a kinesin protein(s) was the reason why AdV replication was inefficient in nc886 KO cells. There are 61 genes in the kinesin family (Table S2). After filtering out 31 kinesin genes whose expression levels are negligible, the expression change of 30 kinesin genes were displayed in a heatmap (Figure 5C and Table S2). Based on their expression levels depending on nc886 as well as KD phenotypes in previous literature,[35] we selected six kinesin genes for RT-qPCR validation. The expression of four kinesin genes (KIF5C, KIF20A, KIF22, and KIF23) was significantly increased in PKR^{KO}:nc886^{KO} cells as compared with PKR^{WT}:nc886^{WT} cells, whereas KIF4A and KIF4B did not change significantly (Figure S5). Among the four, we chose KIF20A and KIF22 for the next KD experiments, because they were expressed more abundantly or increased more remarkably than the other two. Transfection of siRNAs against KIF20A and KIF22 (in one mixture) efficiently decreased their expression and, importantly, rescued the AdV nuclear entry and replication in nc886 KO cells to a significant degree (Figure 5D). Conclusively, suppression of kinesin motor proteins, particularly KIF20A and KIF22, and consequent facilitation of AdV trafficking to the nucleus were the mechanism how nc886 played a stimulating role in the AdV life cycle.

nc886, which is conserved in most primates and some other mammals, promotes AdV when expressed in mouse cells

There is a notion that replication of human AdV is restricted in human cells.[8] However, several reports showed replication of human AdV in non-primate species such as pig, tree shrew, and dog (Jogler et al[16] Li et al[38] Ternovoi et al[39]; see Figure 6A and Table S3). In addition, human AdV appears to replicate in non-human primates. A number of AdV isolates from several primates are highly homologous in sequence, indicating the zoonotic transmission of AdV among primate species such as human, chimpanzee, gorilla, baboon, monkey, and macaque (Wevers et al[40] Roy et al[41] Medkour et al[42]; see Figure 6A).

The nc886 gene is evolutionarily conserved in most primates and several non-primate species in the class Mammalia (Stadler et al[43]; Figure 6A and Table S3). We surveyed existence of the nc886 gene in the aforementioned animal species and compared with their permissiveness to human AdV. Albeit with few exceptions, such as pigs and guinea pigs, those possessing the nc886 gene mostly tended to be permissive to human AdV (Figure 6A).

The mouse genome does not seem to have the nc886 gene, according to a previous report.[43] In that report, the authors searched the nc886 gene in various animal species based on sequence homology to vault RNAs (vtRNAs) and classified nc886 (also known as vtRNA2-1) as one of them. Nonetheless, we clearly demonstrated that nc886 is functionally distinct from canonical vtRNAs (vtRNA1-1, 1–2, and 1–3 in humans).[17] In all animal species where the nc886 gene exists, it is located between TGFBI and SMAD5. Stadler et al failed to find a sequence homologous to vtRNAs in the mouse genomic region spanning Tgfbi and Smad5.[43] Since the sequence-based *in silico* search was so far the only evidence for the absence of nc886 in mice, we wanted to ascertain this by looking into high-throughput RNA-sequencing (RNA-seq) data. No RNA-seq read was captured in this region (Figures 6B and S6A). For comparison, we could detect RNA-seq reads for Rpph1 and Vaultrc5 (the murine ortholog of canonical vtRNAs), which are both transcribed by Pol III (Figures S6B and S6C). Furthermore, we rummaged the Tgfbi-Smad5 region but could not see any vestige of a Pol III gene, such as an A/B box and an oligo-T stretch, which are the promoter and termination elements for Pol III transcription. Collectively, we reassured that nc886 was not conserved in mice.

Several studies showed that mouse cells do not support the complete life cycle of human AdV.[13–16] This impeded the development of a mouse model to evaluate the utility of human AdV *in vivo*. We questioned whether introduction of nc886 into mouse cells promotes the propagation of human AdV. We had generated an nc886-expressing derivative from RAW 264.7 mouse macrophage cell line ("RAW:nc886" and a control cell line "RAW:vector"[26]). We infected AdV into these cell lines and found AdV DNA replication, gene expression, and released AdV amount to be elevated when nc886 was expressed (Figures 6C–6E). These data indicated that nc886 promotes human AdV replication and gene expression, when xenogeneically expressed in mice. Among many differences between humans and mice, nc886 could be one reason why mouse cells do not support human AdV replication.

DISCUSSION

In this study we identified nc886 to be a crucial factor in the AdV infection cycle. Albeit a host ncRNA, nc886 helped AdV replication

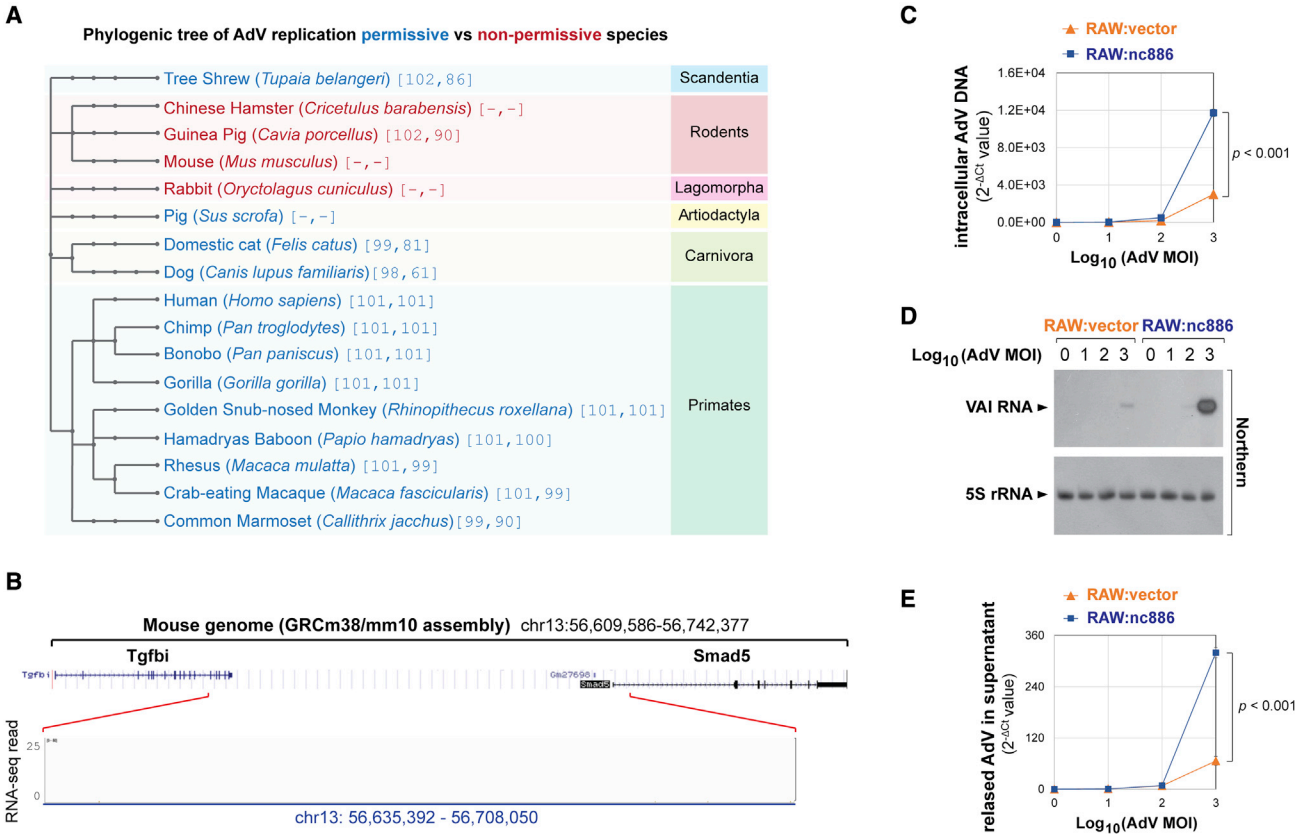

Figure 6. nc886 promotes AdV gene expression and replication when ectopically expressed in a mouse cell line

(A) A phylogenetic tree of a collection of mammalian species whose information on AdV permissiveness and nc886 status are available. AdV-permissive species and non-permissive species are distinguished by blue and red letters respectively. Information on the nc886 gene in nucleotides is indicated in square bracket in this way [length of the nc886 gene in indicated species, the number of matched nucleotides to the human nc886]. No conservation of the nc886 gene is designated as [-, -]. (B) The mouse genomic locus spanning Tfgbi and Smad5 genes. The cartoon has been edited from the UCSC genome browser view and the IGV sequence view, with addition of informative captions. The sequence view portion is blank, indicative of no sequence read captured (see Figure S6 for comparison). (C–E) qPCR of intracellular replicated AdV DNA (C), northern of VAI RNA and 5S rRNA for equal loading (D), and qPCR of released AdV DNA (E), at 24 h post-infection of AdV at indicated MOIs. All other descriptions are the same as Figures 3B, 3C, and 2B.

and gene expression, by facilitating the nuclear entry of AdV (Figure 7). In addition, we demonstrated that PKR was not essential for the stimulatory role of nc886 on AdV. Our data also showed that PKR deficiency *per se* barely took effect on AdV.

Our study has discovered a novel mechanism for a host ncRNA to promote a virus. A host ncRNA confers a milieu for favorable trafficking to the nucleus upon AdV. When we looked into the magnitude of the impact of nc886, the beginning was weak but the end was prosperous. When nc886 was absent, the nuclear import of AdV and its direct consequence, transcription of the immediate-early gene, was only about 2-fold lower. In comparison, AdV DNA replication, and subsequent events accordingly, were almost abrogated in nc886-deficient cells. One possibility is that the initial modest difference has been amplified, similar to the butterfly effect. Alternatively, nc886 might provide AdV with additional favor at a step(s) from transcription of early genes until AdV DNA replication.

Our finding that PKR KO had barely an effect on AdV propagation was against initial anticipation, given the established role of PKR in antiviral responses. During the AdV infection cycle, PKR activity displays two waves of activation and repression, one at a very early time point (~90 min) and the other at the time point of DNA replication (~18 h).[44] It has been shown that PKR activity is suppressed by VA RNAs[45,46] as well as by AdV E1B-55K and E4orf6 proteins.[44] During *in vitro* infection at high AdV dose, those PKR-inhibitory genes will be expressed at a sufficient level to well suppress PKR activity. This might be a reason why AdV infection was equally efficient regardless of PKR WT or KO. We also speculate that PKR suppression by nc886 might be needed in natural situations when a limited amount of AdV infects a cell.

An interesting observation was deprivation of nc886 by AdV, whose significance deserves further discussion in the point of PKR regulation, although the stimulatory effect of nc886 on AdV was

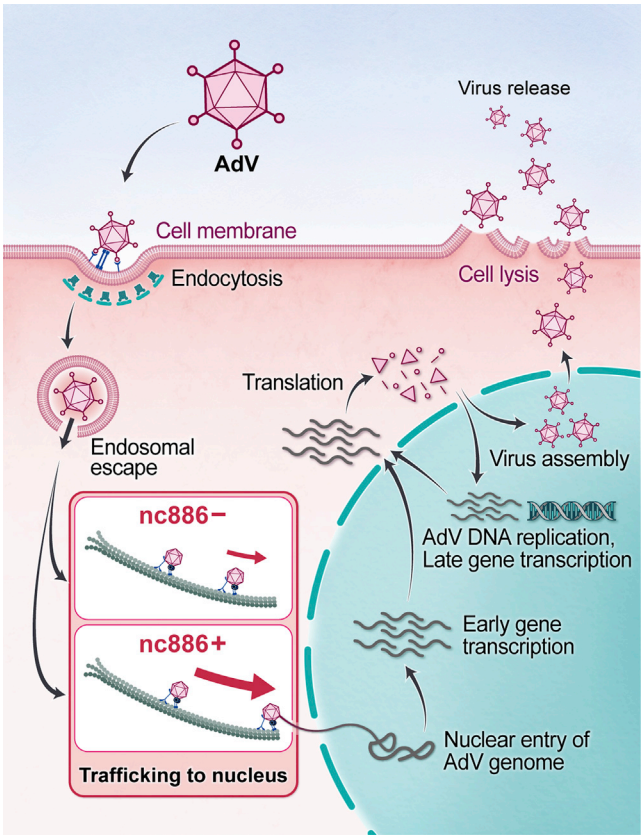

Figure 7. Cartoon depicting the role of nc886 in the AdV life cycle

independent of PKR. nc886 deprivation might be the genuine trigger of the late activation of PKR at ~18 h. Despite the frustration of PKR activation by AdV genes, nc886 deprivation might still be another device for cells to evoke innate immune responses. Besides PKR, nc886 inhibits Interferon Regulatory Factor 3 (IRF3) via Mitochondrial AntiViral-Signaling protein (MAVS) to suppress the interferon response.[26]

Our finding is of clinical importance in several aspects. nc886 is transcribed by Pol III. During tumorigenesis, Pol III activity is generally elevated and accordingly nc886 expression is usually higher in cancer cells than normal quiescent cells.[18] However, nc886 expression is epigenetically silenced in a subset of cancer cells[47] or declines abruptly during chemotherapy.[48] Our key finding here, that AdV replication and the cytotoxicity were inefficient in the absence of nc886, provides an explanation of why oncolytic virotherapy is not effective for all cancer patients.[12] Our study warrants a need to determine the nc886 status, when designing oncolytic virotherapy for a patient. In case of nc886-silenced tumor cells, co-administration of nc886 might improve the oncolytic efficacy of AdV. In-depth understanding of the interplay between AdV genes and nc886 (and related pathways) should precede harnessing nc886 or engineering AdV for therapeutic purposes.

Another significance of our study lies in the mouse cell data (Figure 6). Inefficient replication of human AdV in mice and other animal species hampered the development of an animal model for preclinical studies in which safety and efficacy of a therapeutically engineered AdV are to be evaluated. Since we found that the pro-AdV role of nc886 operates when xenogeneically expressed, construction of an nc886-expressing transgenic animal would be a choice when we are to ameliorate an *in vivo* model system for AdV.

Although AdV is renowned for its clinical utility, the natural pathology of AdV cannot be ignored. Although infection of naturally occurring AdV usually causes mild symptoms and is self-limiting, it can be fatal to immune-deficient individuals. Yet, there is no effective drug for the treatment of AdV infection until now (reviewed in Hendrickx et al[49]). Our data suggest that inhibition of nc886 by administration of an oligonucleotide targeting nc886 might provide a treatment option.

MATERIALS AND METHODS

Cell lines, AdVs, antibodies, and other reagents

Cell lines were purchased from American Type Culture Collection (ATCC; Manassas, VA) or our laboratory stock. Cells were tested for mycoplasma contamination at the Genomics Core in the National Cancer Center, Korea, and were confirmed to be devoid of it. The plasmid "pLL3.7.Puro.U6" was modified from a lentiviral vector pLL3.7 (Addgene; Watertown, MA) by replacing GFP with the puromycin-resistance gene. We constructed an nc886-expressing plasmid by inserting a 102-nucleotide long DNA fragment corresponding to the nc886 RNA region[17] into lentiviral vector pLL3.7.puro.U6. This construct and pLL3.7.puro.U6 were used to construct nc886-expressing and control cell lines from original UM-SCC-19 and RWPE-1. Preparation of lentiviruses, infection onto cells, and subsequent steps to isolate cell clones were according to standard laboratory protocols. Nthy-ori 3-1 WT and KO cell lines are described in Lee et al[29] nc886-expressing and control cell lines derived from RAW264.7 (designated "RAW:nc886" and "RAW:vector") are described in Lee et al.[26]

AdV5 is a WT human AdV (species C serotype 5, accession number AY339865.1)[50] and was obtained from ATCC (VR-1516). Ad5/35CMV-GFP was our laboratory stock and constructed as described in Do et al.[30] AdV virions were propagated in HEK293 cells and purified by using Adeno-X Maxi Purification Kit (Takara Bio USA, Inc., Mountain View, CA) or by the CsCl method as previously described.[50] Our standard procedure for AdV infection was as follows: addition of AdV at indicated multiplicity of infection (MOI) in serum-free medium, incubation for 2 h, and then replacement with medium containing 10% fetal bovine serum.

Hexon and GAPDH antibodies were purchased from Merck Millipore (Burlington, MA) and Cell Signaling Technology, Inc. (Danvers, MA). Total PKR antibody was from Abcam (Cambridge, MA). AdV protein VII antibody was a mouse monoclonal antibody generated and kindly provided by Wodrich laboratory.[51]

AdV DNA and RNA measurement

Total RNA from cells was isolated by Trizol reagent (Life Technologies, Carlsbad, CA). Northern hybridization was done as previously described.[17] cDNA was synthesized by amfiRivert kit (GenDEPOT; Barker, TX) and real-time PCR was done with LightCycler 480 SYBR Green I MasterMix (Roche; Penzberg, Germany) and LightCycler 480 Instrument II (Roche). When AdV mRNAs and pre-mRNAs were measured, two tactics were employed to ensure that the PCR amplification was from RNA but not from AdV DNA. First, prepared RNA was treated with DNase I (New England Biolabs; Ipswich, MA). Second, a reaction without reverse transcriptase ("no RT reaction") was done in parallel with a cDNA synthesis reaction ("+ RT reaction"). A PCR value from "no RT reaction" was used as a baseline for the corresponding value of "+ RT reaction." AdV DNA within infected cells was measured by qPCR directly on isolated nucleic acids by Trizol without cDNA synthesis. AdV DNA in AdV virions released from cells was measured by qPCR of 3 μL of culture supernatant, which had been 8-fold diluted in Tris-EDTA buffer. In all graphs for AdV DNA PCR data, we displayed 2^{-Ct} values relative to uninfected samples, for which sampling and qPCR were performed in parallel. Primer and probe sequences are summarized in Table S4.

Cell viability assay

We assessed the cytopathic effect of AdV on infected cells as performed in O-Carroll et al[52]: 1×10^4 cells were seeded in a 96-well plate and incubated overnight. Cells were infected with AdV at indicated MOIs for 72 h and then floating cells were removed by aspiration. The protein content of attached cells was measured by adding 100 μL of Pierce BCA protein assay reagent (Thermo Fisher Scientific, Waltham, MA) to each well. The subsequent steps were according to the manufacturer's instructions. The protein content was measured by the absorbance at 570 nm. We performed the same BCA assay with 96 wells containing serially diluted uninfected cells, to plot a standard curve from which we converted an absorbance value to a cell density.

IF for AdV protein VII

Cells were cultured on a 12-well plate containing coverslips (18-mm diameter) coated with poly-L-lysine. Cells were infected with AdV at 50 MOI for the indicated hours and were fixed for 10 min with 4% formaldehyde in PBS. Fixed cells were exposed for 30 min at room temperature to PBS containing 0.1% Triton X-100 and 5% horse serum (Gibco-BRL, Thermo Fisher Scientific), and were incubated overnight at 4°C with primary antibody in the same solution, washed three times with PBS, and were incubated for 30 min at room temperature with Alexa Fluor 488–conjugated secondary antibody (Molecular Probes, Thermo Fisher Scientific). Cells were also treated with DAPI (0.2 μg/mL) to stain nuclei.

Assays for AdV attachment to cells, internalization, and nuclear entry

AdV particles that were attached on the cell surface and had entered within cells were measured by "attachment assay" and "internalization assay," respectively; 2×10^5 cells were seeded in a 6-well plate and incubated overnight. Cells were incubated at 4°C for 30 min prior to infection, then infected with AdV at 10 MOI, and further incubated at 4°C for 1 h. After washing three times with ice-cold PBS, cells in a well were harvested by scrapping for attachment assay. Cells in another well were further proceeded for internalization assay, by incubation at 37°C in fresh medium for 1 h. Cells were washed with PBS three times and harvested by trypsinization. Harvested cell pellets were again washed three times with PBS. These extensive wash steps were to remove AdV particles attached on the cell surface. DNA was isolated from harvested cells, by DNeasy Blood & Tissue Kit (Qiagen, Germantown, MD). AdV DNA amount was quantified by qPCR and normalized to qPCR values of cellular 18S rDNA.

Subcellular fractionation was performed to isolate nuclei from cytosolic fractions, as described in Lee et al,[17] with minor modifications at a washing step and buffer composition. After cell lysis, nuclear pellets were washed twice (once in the original protocol) to ensure complete elimination of contaminating cytoplasmic fraction and AdV particles on the nuclear surface. We also omitted RNase inhibitors from all buffers, since they were dispensable for AdV DNA measurement.

Antisense oligonucleotides, siRNA, and transfection

Modified antisense oligonucleotides (anti-oligos) for nc886 KD experiments ("anti-nc886" and "anti-control") in this study were the same as our previous study.[17,26] siRNAs targeting kinesins were Stealth RNAi siRNA from Invitrogen (Carlsbad, CA). Their targeting sequences are 5′-cagugcaaagcagagcuaaacucua-3′ (for KIF20A) and 5′-cgacgcagcagaggcgacgcgagau-3′ (for KIF22). Small RNAs, at 100 nM (for anti-oligos) or 40 nM (for siRNAs), were transfected using Lipofectamine RNAiMAX Reagent (Invitrogen) per the manufacturer's instruction.

Statistical analysis

Unless specified otherwise in the figure legends, statistical significance in most experiments (PCR, GFP, and IF quantification, etc.) was indicated by p values that were calculated from triplicate samples by using unpaired Student's t test.

SUPPLEMENTAL INFORMATION

Supplemental information can be found online at https://doi.org/10.1016/j.omto.2022.02.018.

ACKNOWLEDGMENTS

We thank Dr. Harald Wodrich (Université de Bordeaux, France) for an antibody against AdV protein VII. The illustration (Figure 7) was supported by Suhyun Chae from National Cancer Center Korea. This work was supported by grants from the National Research Foundation of Korea funded by the Korea government (Ministry of Science and ICT; MSIT) (NRF-2019R1A2C2088108 to Y.S.L.); the National Cancer Center, Korea (NCC-2110191 to Y.S.L. and NCC-2110192 to I.-H.K.); the Collaborative Genome Program for Fostering New Post-Genome Industry of the National Research Foundation funded

by the Ministry of Science and ICT (MSIT) (NRF-2017M3C 9A6044517 to Y.-S.L.); International Cooperation & Education Program of National Cancer Center (NCCRI·NCCI 52210-52211, 2021 to E.S.); and the Korea Basic Science Institute (National Research Facilities and Equipment Center) funded by the Ministry of Education (2019R1A6C1010020 to D.K.).

AUTHOR CONTRIBUTIONS

E.S.: Data curation, Formal Analysis, Funding acquisition, Investigation, Methodology, Writing – review & editing.
J.P.: Investigation.
D.K.: Data curation, Formal Analysis, Funding acquisition.
S.-P.S.: Investigation.
W.R.I.: Investigation.
H.-H.L.: Investigation.
J.J.J.: Investigation, Formal Analysis.
J.-L.P.: Formal Analysis.
S.-Y.K.: Formal Analysis.
J.-A.H.: Methodology.
Y.-D.K.: Data curation.
J.-H.L.: Data curation.
E.J.P.: Supervision.
Y.-S.L.: Conceptualization, Funding acquisition, Project administration, Writing – review & editing, Investigation.
I.-H.K.: Conceptualization, Funding acquisition, Supervision.
S.-J.L.: Conceptualization, Writing – review & editing, Supervision, Investigation.
Y.S.L.: Conceptualization, Data curation, Formal Analysis, Funding acquisition, Investigation, Project administration, Supervision, Visualization, Writing – original draft, Writing – review & editing.

DECLARATION OF INTERESTS

The authors declare no competing interests.

REFERENCES

1. Jounaidi, Y., Doloff, J.C., and Waxman, D.J. (2007). Conditionally replicating adenoviruses for cancer treatment. Curr. Cancer Drug Targets *7*, 285–301. https://doi.org/10.2174/156800907780618301.

2. Lee, C.S., Bishop, E.S., Zhang, R., Yu, X., Farina, E.M., Yan, S., Zhao, C., Zheng, Z., Shu, Y., Wu, X., et al. (2017). Adenovirus-mediated gene delivery: potential applications for gene and cell-based therapies in the new era of personalized medicine. Genes Dis. *4*, 43–63. https://doi.org/10.1016/j.gendis.2017.04.001.

3. Mennechet, F.J.D., Paris, O., Ouoba, A.R., Salazar Arenas, S., Sirima, S.B., Takoudjou Dzomo, G.R., Diarra, A., Traore, I.T., Kania, D., Eichholz, K., et al. (2019). A review of 65 years of human adenovirus seroprevalence. Expert Rev. Vaccines *18*, 597–613. https://doi.org/10.1080/14760584.2019.1588113.

4. Wolfrum, N., and Greber, U.F. (2013). Adenovirus signalling in entry. Cell. Microbiol. *15*, 53–62. https://doi.org/10.1111/cmi.12053.

5. Pied, N., and Wodrich, H. (2019). Imaging the adenovirus infection cycle. FEBS Lett. *593*, 3419–3448. https://doi.org/10.1002/1873-3468.13690.

6. Ma, Y., and Mathews, M.B. (1996). Structure, function, and evolution of adenovirus-associated RNA: a phylogenetic approach. J. Virol. *70*, 5083–5099. https://doi.org/10.1128/JVI.70.8.5083-5099.1996.

7. Vachon, V.K., and Conn, G.L. (2016). Adenovirus VA RNA: an essential pro-viral non-coding RNA. Virus Res. *212*, 39–52. https://doi.org/10.1016/j.virusres.2015.06.018.

8. Vaillancourt, M.T., Atencio, I., Quijano, E., Howe, J.A., and Ramachandra, M. (2005). Inefficient killing of quiescent human epithelial cells by replicating adenoviruses: potential implications for their use as oncolytic agents. Cancer Gene Ther. *12*, 691–698. https://doi.org/10.1038/sj.cgt.7700840.

9. Critchley-Thorne, R.J., Simons, D.L., Yan, N., Miyahira, A.K., Dirbas, F.M., Johnson, D.L., Swetter, S.M., Carlson, R.W., Fisher, G.A., Koong, A., et al. (2009). Impaired interferon signaling is a common immune defect in human cancer. Proc. Natl. Acad. Sci. U S A *106*, 9010–9015. https://doi.org/10.1073/pnas.0901329106.

10. Grander, D., and Einhorn, S. (1998). Interferon and malignant disease–how does it work and why doesn't it always? Acta Oncol. *37*, 331–338. https://doi.org/10.1080/028418698430548.

11. Baker, A.T., Aguirre-Hernandez, C., Hallden, G., and Parker, A.L. (2018). Designer oncolytic adenovirus: coming of age. Cancers (Basel) *10*. https://doi.org/10.3390/cancers10060201.

12. Huebner, R.J., Rowe, W.P., Schatten, W.E., Smith, R.R., and Thomas, L.B. (1956). Studies on the use of viruses in the treatment of carcinoma of the cervix. Cancer *9*, 1211–1218. https://doi.org/10.1002/1097-0142(195611/12)9:6<1211::aid-cncr2820090624>3.0.co;2-7.

13. Duncan, S.J., Gordon, F.C., Gregory, D.W., McPhie, J.L., Postlethwaite, R., White, R., and Willcox, H.N. (1978). Infection of mouse liver by human adenovirus type 5. J. Gen. Virol. *40*, 45–61. https://doi.org/10.1099/0022-1317-40-1-45.

14. Ginsberg, H.S., Moldawer, L.L., Sehgal, P.B., Redington, M., Kilian, P.L., Chanock, R.M., and Prince, G.A. (1991). A mouse model for investigating the molecular pathogenesis of adenovirus pneumonia. Proc. Natl. Acad. Sci. U S A *88*, 1651–1655. https://doi.org/10.1073/pnas.88.5.1651.

15. Young, A.M., Archibald, K.M., Tookman, L.A., Pool, A., Dudek, K., Jones, C., Williams, S.L., Pirlo, K.J., Willis, A.E., Lockley, M., and McNeish, I.A. (2012). Failure of translation of human adenovirus mRNA in murine cancer cells can be partially overcome by L4-100K expression in vitro and in vivo. Mol. Ther. *20*, 1676–1688. https://doi.org/10.1038/mt.2012.116.

16. Jogler, C., Hoffmann, D., Theegarten, D., Grunwald, T., Uberla, K., and Wildner, O. (2006). Replication properties of human adenovirus in vivo and in cultures of primary cells from different animal species. J. Virol. *80*, 3549–3558. https://doi.org/10.1128/JVI.80.7.3549-3558.2006.

17. Lee, K., Kunkeaw, N., Jeon, S.H., Lee, I., Johnson, B.H., Kang, G.Y., Bang, J.Y., Park, H.S., Leelayuwat, C., and Lee, Y.S. (2011). Precursor miR-886, a novel noncoding RNA repressed in cancer, associates with PKR and modulates its activity. RNA *17*, 1076–1089. https://doi.org/10.1261/rna.2701111.

18. Park, J.L., Lee, Y.S., Song, M.J., Hong, S.H., Ahn, J.H., Seo, E.H., Shin, S.P., Lee, S.J., Johnson, B.H., Stampfer, M.R., et al. (2017). Epigenetic regulation of RNA polymerase III transcription in early breast tumorigenesis. Oncogene *36*, 6793–6804. https://doi.org/10.1038/onc.2017.285.

19. Ahn, J.H., Lee, H.S., Lee, J.S., Lee, Y.S., Park, J.L., Kim, S.Y., Hwang, J.A., Kunkeaw, N., Jung, S.Y., Kim, T.J., et al. (2018). nc886 is induced by TGF-beta and suppresses the microRNA pathway in ovarian cancer. Nat. Commun. *9*, 1166. https://doi.org/10.1038/s41467-018-03556-7.

20. Jeon, S.H., Lee, K., Lee, K.S., Kunkeaw, N., Johnson, B.H., Holthauzen, L.M., Gong, B., Leelayuwat, C., and Lee, Y.S. (2012). Characterization of the direct physical interaction of nc886, a cellular non-coding RNA, and PKR. FEBS Lett. *586*, 3477–3484. https://doi.org/10.1016/j.febslet.2012.07.076.

21. Calderon, B.M., and Conn, G.L. (2017). Human noncoding RNA 886 (nc886) adopts two structurally distinct conformers that are functionally opposing regulators of PKR. RNA *23*, 557–566. https://doi.org/10.1261/rna.060269.116.

22. Golec, E., Lind, L., Qayyum, M., Blom, A.M., and King, B.C. (2019). The noncoding RNA nc886 regulates PKR signaling and cytokine production in human cells. J. Immunol. *202*, 131–141. https://doi.org/10.4049/jimmunol.1701234.

23. Mrazek, J., Kreutmayer, S.B., Grasser, F.A., Polacek, N., and Huttenhofer, A. (2007). Subtractive hybridization identifies novel differentially expressed ncRNA species in EBV-infected human B cells. Nucleic Acids Res. *35*, e73. https://doi.org/10.1093/nar/gkm244.

24. Nandy, C., Mrazek, J., Stoiber, H., Grasser, F.A., Huttenhofer, A., and Polacek, N. (2009). Epstein-barr virus-induced expression of a novel human vault RNA. J. Mol. Biol. *388*, 776–784. https://doi.org/10.1016/j.jmb.2009.03.031.

25. Li, F., Chen, Y., Zhang, Z., Ouyang, J., Wang, Y., Yan, R., Huang, S., Gao, G.F., Guo, G., and Chen, J.L. (2015). Robust expression of vault RNAs induced by influenza A virus plays a critical role in suppression of PKR-mediated innate immunity. Nucleic Acids Res. *43*, 10321–10337. https://doi.org/10.1093/nar/gkv1078.

26. Lee, Y.S., Bao, X., Lee, H.H., Jang, J.J., Saruuldalai, E., Park, G., Im, W.R., Park, J.L., Kim, S.Y., Shin, S., et al. (2021). Nc886, a novel suppressor of the type I interferon response upon pathogen intrusion. Int. J. Mol. Sci. *22*. https://doi.org/10.3390/ijms22042003.

27. Kunkeaw, N., Jeon, S.H., Lee, K., Johnson, B.H., Tanasanvimon, S., Javle, M., Pairojkul, C., Chamgramol, Y., Wongfieng, W., Gong, B., et al. (2013). Cell death/proliferation roles for nc886, a non-coding RNA, in the protein kinase R pathway in cholangiocarcinoma. Oncogene *32*, 3722–3731. https://doi.org/10.1038/onc.2012.382.

28. Im, W.R., Lee, H.S., Lee, Y.S., Lee, J.S., Jang, H.J., Kim, S.Y., Park, J.L., Lee, Y., Kim, M.S., Lee, J.M., et al. (2020). A regulatory noncoding RNA, nc886, suppresses esophageal cancer by inhibiting the AKT pathway and cell cycle progression. Cells *9*. https://doi.org/10.3390/cells9040801.

29. Lee, E.K., Hong, S.H., Shin, S., Lee, H.S., Lee, J.S., Park, E.J., Choi, S.S., Min, J.W., Park, D., Hwang, J.A., et al. (2016). nc886, a non-coding RNA and suppressor of PKR, exerts an oncogenic function in thyroid cancer. Oncotarget *7*, 75000–75012. https://doi.org/10.18632/oncotarget.11852.

30. Do, M.H., To, P.K., Cho, Y.S., Kwon, S.Y., Hwang, E.C., Choi, C., Cho, S.H., Lee, S.J., Hemmi, S., and Jung, C. (2018). Targeting CD46 enhances anti-tumoral activity of adenovirus type 5 for bladder cancer. Int. J. Mol. Sci. *19*. https://doi.org/10.3390/ijms19092694.

31. Punga, T., Darweesh, M., and Akusjarvi, G. (2020). Synthesis, structure, and function of human adenovirus small non-coding RNAs. Viruses *12*. https://doi.org/10.3390/v12101182.

32. Sohn, S.Y., and Hearing, P. (2019). Adenoviral strategies to overcome innate cellular responses to infection. FEBS Lett. *593*, 3484–3495. https://doi.org/10.1002/1873-3468.13680.

33. Greber, U.F., and Flatt, J.W. (2019). Adenovirus entry: from infection to immunity. Annu. Rev. Virol. *6*, 177–197. https://doi.org/10.1146/annurev-virology-092818-015550.

34. Zheng, K., Kitazato, K., and Wang, Y. (2014). Viruses exploit the function of epidermal growth factor receptor. Rev. Med. Virol. *24*, 274–286. https://doi.org/10.1002/rmv.1796.

35. Zhou, J., Scherer, J., Yi, J., and Vallee, R.B. (2018). Role of kinesins in directed adenovirus transport and cytoplasmic exploration. PLoS Pathog. *14*, e1007055. https://doi.org/10.1371/journal.ppat.1007055.

36. Berry, G.E., and Tse, L.V. (2017). Virus binding and internalization assay for adeno-associated virus. Bio Protoc. *7*. https://doi.org/10.21769/BioProtoc.2110.

37. Hirokawa, N., Noda, Y., Tanaka, Y., and Niwa, S. (2009). Kinesin superfamily motor proteins and intracellular transport. Nat. Rev. Mol. Cell Biol. *10*, 682–696. https://doi.org/10.1038/nrm2774.

38. Li, X., Zhou, Z., Liu, W., Fan, Y., Luo, Y., Li, K., Zheng, Z., Tian, X., and Zhou, R. (2021). Chinese tree shrew: a permissive model for in vitro and in vivo replication of human adenovirus species B. Emerg. Microbes Infect. *10*, 424–438. https://doi.org/10.1080/22221751.2021.1895679.

39. Ternovoi, V.V., Le, L.P., Belousova, N., Smith, B.F., Siegal, G.P., and Curiel, D.T. (2005). Productive replication of human adenovirus type 5 in canine cells. J. Virol. *79*, 1308–1311. https://doi.org/10.1128/JVI.79.2.1308-1311.2005.

40. Wevers, D., Metzger, S., Babweteera, F., Bieberbach, M., Boesch, C., Cameron, K., Couacy-Hymann, E., Cranfield, M., Gray, M., Harris, L.A., et al. (2011). Novel adenoviruses in wild primates: a high level of genetic diversity and evidence of zoonotic transmissions. J. Virol. *85*, 10774–10784. https://doi.org/10.1128/JVI.00810-11.

41. Roy, S., Vandenberghe, L.H., Kryazhimskiy, S., Grant, R., Calcedo, R., Yuan, X., Keough, M., Sandhu, A., Wang, Q., Medina-Jaszek, C.A., et al. (2009). Isolation and characterization of adenoviruses persistently shed from the gastrointestinal tract of non-human primates. PLoS Pathog. *5*, e1000503. https://doi.org/10.1371/journal.ppat.1000503.

42. Medkour, H., Amona, I., Akiana, J., Davoust, B., Bitam, I., Levasseur, A., Tall, M.L., Diatta, G., Sokhna, C., Hernandez-Aguilar, R.A., et al. (2020). Adenovirus infections in african humans and wild non-human primates: great diversity and cross-species transmission. Viruses *12*. https://doi.org/10.3390/v12060657.

43. Stadler, P.F., Chen, J.J., Hackermuller, J., Hoffmann, S., Horn, F., Khaitovich, P., Kretzschmar, A.K., Mosig, A., Prohaska, S.J., Qi, X., et al. (2009). Evolution of vault RNAs. Mol. Biol. Evol. *26*, 1975–1991. https://doi.org/10.1093/molbev/msp112.

44. Spurgeon, M.E., and Ornelles, D.A. (2009). The adenovirus E1B 55-kilodalton and E4 open reading frame 6 proteins limit phosphorylation of eIF2alpha during the late phase of infection. J. Virol. *83*, 9970–9982. https://doi.org/10.1128/JVI.01113-09.

45. O'Malley, R.P., Mariano, T.M., Siekierka, J., and Mathews, M.B. (1986). A mechanism for the control of protein synthesis by adenovirus VA RNAI. Cell *44*, 391–400.

46. Kitajewski, J., Schneider, R.J., Safer, B., Munemitsu, S.M., Samuel, C.E., Thimmappaya, B., and Shenk, T. (1986). Adenovirus VAI RNA antagonizes the antiviral action of interferon by preventing activation of the interferon-induced eIF-2 alpha kinase. Cell *45*, 195–200. https://doi.org/10.1016/0092-8674(86)90383-1.

47. Lee, Y.S. (2015). A novel type of non-coding RNA, nc886, implicated in tumor sensing and suppression. Genom. Inform. *13*, 26–30. https://doi.org/10.5808/GI.2015.13.2.26.

48. Kunkeaw, N., Lee, Y.S., Im, W.R., Jang, J.J., Song, M.J., Yang, B., Park, J.L., Kim, S.Y., Ku, Y., Kim, Y., et al. (2019). Mechanism mediated by a noncoding RNA, nc886, in the cytotoxicity of a DNA-reactive compound. Proc. Natl. Acad. Sci. U S A *116*, 8289–8294. https://doi.org/10.1073/pnas.1814510116.

49. Hendrickx, R., Stichling, N., Koelen, J., Kuryk, L., Lipiec, A., and Greber, U.F. (2014). Innate immunity to adenovirus. Hum. Gene Ther. *25*, 265–284. https://doi.org/10.1089/hum.2014.001.

50. Nam, J.K., Lee, M.H., Seo, H.H., Kim, S.K., Lee, K.H., Kim, I.H., and Lee, S.J. (2010). The development of the conditionally replication-competent adenovirus: replacement of E4 orf1-4 region by exogenous gene. J. Gene Med. *12*, 453–462. https://doi.org/10.1002/jgm.1457.

51. Komatsu, T., Dacheux, D., Kreppel, F., Nagata, K., and Wodrich, H. (2015). A method for visualization of incoming adenovirus chromatin complexes in fixed and living cells. PLoS One *10*, e0137102. https://doi.org/10.1371/journal.pone.0137102.

52. O'Carroll, S.J., Hall, A.R., Myers, C.J., Braithwaite, A.W., and Dix, B.R. (2000). Quantifying adenoviral titers by spectrophotometry. Biotechniques *28*, 408–410. 412. https://doi.org/10.2144/00283bm03.